

The intermediate-age globular cluster NGC 1783 in the Large Magellanic Cloud

Alessio Mucciarelli

Dipartimento di Astronomia, Università degli Studi di Bologna, Via Ranzani, 1 - 40127 Bologna, ITALY

alessio.mucciarelli@studio.unibo.it

Livia Origlia

INAF - Osservatorio Astronomico di Bologna, Via Ranzani, 1 - 40127 Bologna, ITALY

livia.origlia@oabo.inaf.it

Francesco R. Ferraro

Dipartimento di Astronomia, Università degli Studi di Bologna, Via Ranzani, 1 - 40127 Bologna, ITALY

francesco.ferraro3@unibo.it

ABSTRACT

We present *Hubble Space Telescope* ACS deep photometry of the intermediate-age globular cluster NGC 1783 in the Large Magellanic Cloud. By using this photometric dataset, we have determined the degree of ellipticity of the cluster ($\epsilon=0.14\pm 0.03$) and the radial density profile. This profile is well reproduced by a standard King model with an extended core ($r_c=24.5''$) and a low concentration ($c=1.16$), indicating that the cluster has not experienced the collapse of the core.

We also derived the cluster age, by using the *Pisa Evolutionary Library* (PEL) isochrones, with three different amount of *overshooting* (namely, $\Lambda_{os}=0.0, 0.10$ and 0.25). From the comparison of the observed Color-Magnitude Diagram (CMD) and Main Sequence (MS) Luminosity Function (LF) with the theoretical isochrones and LFs, we find that only models with the inclusion of some *overshooting* ($\Lambda_{os}=0.10-0.25$) are able to reproduce the observables. By using the magnitude difference $\delta V_{SGB}^{He-Cl} = 0.90$ between the mean level of the He-clump and the flat region of the SGB, we derive an age $\tau=1.4\pm 0.2$ Gyr.

Subject headings: Magellanic Clouds — globular clusters: individual (NGC 1783) — techniques: photometry

1. Introduction

Stellar clusters are key-tracers of stellar populations in different galactic environments. In particular, populous clusters in the Large Magellanic Cloud (LMC) cover a wide range of ages (from a few Myr up to 13 Gyr) which has no counterpart in our Galaxy. Hence, the study of this system allows to extend our empirical knowledge of stellar populations in a mass regime which can be poorly explored in our Galaxy.

The LMC clusters can be grouped in three main age families, namely: the young population with ages ≤ 200 Myr (Vallenari et al. 1994; Testa et al. 1999), the intermediate population in the $200 \text{ Myr} < \text{age} < 3\text{-}4 \text{ Gyr}$ range (Ferraro et al. 1995; Brocato et al. 2001; Gallart et al. 2003; Ferraro et al. 2004a) and the old population, with stellar clusters coeval to the Galactic Halo ones (Testa et al. 1995; Brocato et al. 1996; Olsen et al. 1998; Mackey & Gilmore 2004).

A few decades ago, the main integrated properties of the LMC cluster system, both in the infrared (Persson et al. 1983) and in the optical (Mould & Aaronson 1979, 1982; Searle, Wilkinson, & Bagnuolo 1980; van den Bergh 1981) spectral ranges have been investigated. These studies also provided the only existent homogeneous age-scale, based on the so-called *s-parameter*, as defined by Elson & Fall (1985). This parameter is an empirical quantity related to the position of the clusters in the (U-B)-(B-V) color-color diagram. Clearly, this method presents many uncertainties, namely the foreground/background contamination and the possible statistical fluctuations due to bright stars.

The advent of 8-meter class ground-based telescopes and the superior performances of the Hubble Space Telescope (HST) provide sufficient resolution to properly study these clusters even in their innermost crowded regions. Accurate ages can be determined from the Main Sequence (MS) Turn-Off (TO) measurements (see e.g. the recent works by Mackey, Payne & Gilmore 2006; Kerber, Santiago & Brocato 2007; Mucciarelli et al. 2007), once updated theoretical evolutionary models are adopted and precise estimates of the global metallicity (Salaris et al. 1993) be available. Indeed, the stellar clock is extremely sensitive to the chemical composition and detailed abundances of iron and α -elements from high-resolution spectroscopy are mandatory for this purpose.

A few years ago, we started a long term project aimed at determining homogeneous ages and metallicities for a representative sample of template LMC clusters, by combining high-resolution photometry and spectroscopy. The first cluster analyzed so far is NGC 1978: an accurate metallicity of $[\text{Fe}/\text{H}] = -0.37 \pm 0.07$ dex (Ferraro et al. 2006) and an age of $\tau = 1.9 \pm 0.1$ Gyr (Mucciarelli et al. 2007, hereafter Paper I) have been obtained. In this paper we present the results for NGC 1783, another populous intermediate-age cluster. Sect. 2 describes the cluster Color-Magnitude Diagram (CMD) and its main evolutionary features. Sect. 3

describes its structural parameters, while Sect. 4 discusses its age determination. In Sect. 5 we draw our conclusions.

2. Observations and data analysis

The results presented in this paper are based on a set of images obtained with the Advanced Camera for Survey (ACS) Wide Field Channel (WFC) that provides a field of view of $\approx 200'' \times 200''$ with a plate scale of 0.05 arcsec/pixel. All the images have been retrieved from the ESO/ST-ECF Science Archive (Proposal ID 9891, Cycle 12), through the F555W and F814W filters, with exposure times of 250 and 170 sec, respectively. The first chip of the ACS-WFC is centered on the cluster center. Fig. 1 shows the the F814W image of the cluster in both the ACS chips.

The photometric reduction was carried out with the *DAOPHOT-II* package (Stetson 1987) by using the Point Spread Function (PSF) fitting method. The final photometric catalog includes almost 40,000 stars, and it has been calibrated in the VEGAMAG photometric system using the prescriptions of Bedin et al. (2005) and astrometrized on the Two-Micron All-Sky Survey (2MASS) photometric system, by cross-correlating the ACS@HST catalog with the infrared catalog presented by Mucciarelli et al. (2006).

2.1. The CMD overall characteristics

Fig. 2 shows the observed CMD using only the ACS chip sampling the cluster core. The useful magnitude range is $17.6 \leq F555W \leq 26$. Indeed, we note that the brightest stars at $F555W < 17.6$, could be in the non-linear regime of the CCD or saturated in their central pixels, making the corresponding magnitudes and colors somewhat uncertain.

The main features of the observed CMD can be summarized as follows:

- (1) The MS extends over more than 6 magnitudes in the F555W band and the TO point is located at $F555W \approx 21.2$ (the identification of the TO magnitude was done by means of a parabolic fit of this region). The TO region shows a mild spread in color;
- (2) the slope change of the MS is at $F555W \approx 22.2$ and flags the transition between radiative and convective core stellar structures;
- (3) the Sub Giant Branch (SGB) is a poorly populated sequence, with a typical $F555W \approx 20.5$ magnitude. We note that the blue edge of this sequence is not well-defined;
- (4) the Red Giant Branch (RGB) is well populated and it extends over ≈ 5 magnitudes;
- (5) the Helium-Clump is located at $F555W \approx 19.25$ and $(F555W - F814W) \approx 1.15$;
- (6) the Asymptotic Giant Branch (AGB) Clump (corresponding to the base of the AGB

sequence) is visible at $F555W \approx 18.4$.

Fig. 3 shows the radial CMDs by using the entire sample of stars detected in the ACS FoV. The bulk of the cluster population lies in the central 2 arcmin (by radius); at $r > 130''$ the SGB, RGB and He-Clump are barely detectable, while the brightest portion of the cluster MS is still visible.

The mild color broadening of the TO region deserves a brief discussion. Recently, Bertelli et al. (2003) found a color dispersion in the brightest portion of the MS of NGC 2173, while Mackey & Broby Nielsen (2007) found a bifurcation of the bright MS region of NGC 1846, and interpreted it as a double TO. These two observational evidences suggest the possible existence of an age-dispersion in these stellar clusters. In order to check whether the broadening of the TO region in NGC 1783 can be ascribed to a possible age-dispersion as well, we calculated the color distribution of the MS stars in the $20.5 < F555W < 21.1$ magnitude range. The color distribution turns out to be roughly Gaussian with $\sigma_{F555W-F814W} \approx 0.05$, which is fully consistent with the observational errors ($\sigma_{F555W} \sim \sigma_{F814W} \approx 0.03$, implying a color uncertainty $\sigma_{F555W-F814W} \approx 0.04$). Similar results are obtained by computing the color distribution in the radial CMDs of Fig. 3. Thus, we can conclude that the spread in color of the TO region in NGC 1783 can be explained in terms of photometric errors and there is not any evidence of an age-dispersion.

2.2. Completeness

In order to quantify the degree of completeness of the final photometric catalog, we used the well-know artificial star technique (Mateo 1988), and we simulated a population of stars in the same magnitude range covered by the observed CMD (excluding stars brighter than $F555W = 17.6$, corresponding to the saturation level) and with a $(F555W - F814W) \sim 0.8$ mean color. The artificial stars have been added to the original images and the entire data reduction procedure has been repeated using the *enriched* images. The number of artificial stars simulated in each run ($\sim 2,000$) is always a small percentage ($\sim 5\%$) of the detected stars, hence they do not alter the original crowding conditions. A total of ~ 250 runs were performed and more than 500,000 stars have been simulated. We have excluded from our analysis the very inner region of the cluster ($r < 20''$), where the crowding conditions are prohibitive. Fig. 4 shows the completeness factor $\phi = \frac{N_{rec}}{N_{sim}}$, defined as the fraction of recovered stars over the total simulated ones, as a function of the $F555W$ magnitude in two different radial regions, namely between $20''$ and $50''$ and at $r > 50''$ from the cluster center, respectively. In the inner region the sample is $>90\%$ complete down to $F555W \approx 22.5$, while in the outer region is $>90\%$ complete down to $F555W \approx 24$.

3. Ellipticity and structural parameters

The knowledge of the position of each star over the entire extension of the cluster (and in particular in the innermost region) allows to compute the center of gravity (C_{grav}) with high precision. In doing this, we applied the procedure described in Montegriffo et al. (1995), averaging the α and δ coordinates of the detected stars with $F555W < 22$, in order to minimize the effects of incompleteness. The C_{grav} of the cluster turns out to be located at $\alpha = 4^h 59^m 09^s.78$ and $\delta = -65^\circ 59' 17''.82$. This finding is in good agreement with our previous determination based on near-IR photometry (Mucciarelli et al. 2006).

We also used the ACS photometry of NGC 1783 to derive new estimates for the cluster ellipticity and structural parameters. The isodensity curves are computed with an adaptive kernel technique, accordingly to the prescription of Fukunaga (1972). We used all the stars in the first chip with $F555W < 22$ in order to minimize incompleteness effects and we fit the isodensity curves with ellipses. Fig.5 shows the cluster map with the isodensity contours (upper panel), the corresponding best fit ellipses (central panel) and their ellipticity as a function of the semi-major axis in arcsec (lower panel). The ellipticity ϵ (defined as $\epsilon = 1 - (b/a)$, where a and b are the major and minor axis of the ellipse, respectively) turns out to be 0.14 ± 0.03 . This value results slightly lower than the previous determinations of Geisler & Hodge (1980) that found an average ellipticity of $\epsilon = 0.19$.

By following the procedure already described in previous papers (see Ferraro et al. 2004b), we also compute the projected density profile of the cluster. The area sampled by the first ACS chip has been divided in 18 concentric annuli, each one centered on C_{grav} and split in four sub-sectors. The number of stars lying in each sub-sector was counted and the mean star density was obtained. The standard deviation was estimated from the variance among the sub-sectors. The radial density profile is plotted in Fig.6. We used the Sigurdsson & Phinney (1995) code in order to compute the family of isotropic single-mass King models. These models are defined by three main parameters, the central potential W_0 , core radius r_c and the concentration $c = \log(r_t)/(r_c)$, where r_t is the tidal radius. Fig. 6 also shows the single-mass King model that best fit the derived density profile. The best-fit model has been selected by using a χ^2 minimization (shown in the lower panel of Fig. 6).

We find $W_0 = 5.5$, $r_c = 24.5''$ and $c = 1.16$, corresponding to a tidal radius $r_t = 5.9'$ ¹. Our estimate of r_c is consistent with the one by Elson (1992) who found $r_c = 20''$. The resulting

¹We underline that the structure of the profile and the corresponding derived parameters does not change if different magnitude limits are adopted.

r_t lies out of the field of view of ACS. In order to properly fit the most external points of the radial profile, the best-fit King model has been combined with a constant background level (corresponding to a density of 350 stars $arcmin^2$), and shown as a horizontal dashed line in Fig. 6.

4. The age of NGC 1783

Young stellar populations (with ages ≤ 300 Myr) are characterized by large convective cores. Theoretical studies (see e.g. the numerical simulations computed by Freytag, Ludwig & Steffen 1996) suggest that the penetration of convective elements into a stable region (*via the Schwarzschild criterion*) can produce non-negligible evolutionary effects. These prediction seem to be confirmed by several works (Becker & Mathews 1983; Barmina, Girardi & Chiosi 2002; Chiosi & Vallenari 2007) which require some amount of *overshooting* in the MS star convective core, in order to reproduce the observed morphologies and stellar counts of young clusters, although this issue is still matter of debate (Testa et al. 1999; Brocato et al. 2003). At variance, in older ($\geq 5-6$ Gyr) stellar populations the growth of large radiative cores tends to erase the possible evolutionary effects of *overshooting*.

Intermediate-age stellar populations like those in NGC 1978 and NGC 1783 LMC stellar clusters represent the transition stage between these two regimes, and thus represent ideal test-bench to study the *overshooting* effects.

4.1. Basic assumptions

In Paper I we performed a detailed comparison of the observed morphology and star counts of NGC 1978 with different set of theoretical models and *overshooting* efficiencies. The best agreement between observations and theoretical predictions was reached with the Pisa Evolutionary Library (PEL).²

Hence, we have used the PEL isochrones to also determine the age of NGC 1783. We select isochrones with $Z=0.008$ (corresponding to $[M/H]=-0.40$ dex, as estimated by Mucciarelli et al.(2007, in preparation) from high-resolution spectroscopy), and with three different amount of *overshooting* efficiency, namely Λ_{os} ³ =0.0 for the canonical isochrones, and

²The PEL isochrones are available at the URL <http://astro.df.unipi.it/SAA/PEL/Z0.html>.

³The overshooting efficiency is parametrized using the mixing length theory (Bohm-Vitense 1958) with $\Lambda_{os}=1/H_p$ (where H_p is pressure scale height) that quantifies the overshoot distance *above* the Schwarzschild

$\Lambda_{os}=0.10$ and 0.25 , representative of mild and strong *overshooting* regimes, respectively.

These theoretical isochrones have been transformed into the observational plane, by means of suitable conversions computed with the code described by Origlia & Leitherer (2000), and convolving the model atmospheres by Bessel, Castelli & Plez (1998) with the ACS filter responses. Guess values of $(m - M)_0=18.50$ (Alves 2004) for the distance modulus and $E(B-V)=0.10$ (Persson et al. 1983) for reddening have been adopted. However, in order to obtain the best fit of the observed sequences we allowed these parameters to vary by $\leq |10|\%$ and $\leq |40|\%$ factors, respectively.

Fig. 7 shows the best-fit solutions for the different values of Λ_{os} , as obtained by matching the following features:

- (1) the magnitude of the He-Clump;
- (2) the magnitude difference between the He-Clump and the flat region of the SGB;
- (3) the difference in color between the TO and the base of the RGB.

As can be seen, the canonical model with $\Lambda_{os}=0.0$ fit the observational features (1) and (2) reasonably well with $(m - M)_0=18.57$, $E(B-V)=0.13$ and $\tau=0.9$ Gyr, but fails to reproduce feature (3).

Fig. 8 (panel (a)) shows a portion of the CMD, as zoomed onto the TO region, with the best-fit ($\tau=0.9$ Gyr) and 0.3 Gyr older ($\tau=1.2$ Gyr) isochrones. The older isochrones better fits feature (3) but predicts a too bright (by ≈ 0.3 magnitudes) He-clump. Moreover, it requires a $(m - M)_0=18.16$ distance modulus, which is definitely too short for the LMC (Alves 2004).

Fig. 8 (panels (b) and (c)) shows a similar comparison for the overshooting models. For the $\Lambda_{os}=0.10$ model (panel (b)), the best-fit ($\tau=1.2$ Gyr) and 0.2 Gyr older ($\tau=1.4$ Gyr) isochrones are plotted. As for the canonical model, the older isochrones somewhat better fits feature (3) but predicts a too bright (by ≈ 0.25 magnitudes) He-clump and a too short $(m - M)_0=18.25$ distance modulus.

For the $\Lambda_{os}=0.25$ model (panel (c)), the best-fit ($\tau=1.6$ Gyr) and 0.2 Gyr younger ($\tau=1.4$ Gyr) isochrones are shown. The younger isochrone slightly better fits the SGB region but predicts a too blue MS. Also it predicts a slightly too faint (by ≈ 0.2 magnitudes) He-clump and too long $(m - M)_0=18.66$ distance modulus.

In summary, we can conclude that canonical models, regardless the adopted isochrone age, do not provide an acceptable fit to the observed CMD, while models with $\Lambda_{os}=0.10$ and 0.25 *overshooting*, $E(B-V)=0.13$, $(m - M)_0=18.45$ and ages between $\tau=1.2$ and $\tau=1.6$ Gyr, respectively, reasonably well reproduce all the three diagnostics features.

border in units of the pressure scale height.

4.2. Star counts and overshooting efficiency

A quantitative check to discriminate between the different *overshooting scenarios* is to perform a comparison between the observed and theoretical LFs of the MS stars normalized to the number of the He-clump stars, defined as

$$\Phi_{norm} = \lg \frac{\sum_i N_{MS}}{N_{He-Cl}}.$$

Such a normalized LF is a powerful indicator of the relative timescales of the H and He burning phases. The observed Φ_{norm} is obtained by counting the number of MS stars (N_{MS}) in each 0.5 magnitude bin, after the correction for incompleteness and field contamination, and normalized to the total number of He-Clump stars. The innermost region of the cluster ($r < 20''$, see Fig. 3) has been excluded from this analysis because of its prohibitive crowding. Formal errors for the observed Φ_{norm} in each magnitude bin are computed under the assumption that star counts follow the Poisson statistics, by using the following formula:

$$\sigma_{\Phi_{norm}} = \frac{\sqrt{\Phi_{norm}^2 \cdot \sigma_{N_{He-Cl}}^2 + \sigma_{N_{MS}}^2}}{N_{He-Cl}}.$$

Since the ACS field of view is not large enough to properly sample the field population around NGC 1783, we used the most external region ($r > 150''$) of the decontamination field for NGC1978 (Paper I). Indeed, these two clusters are close enough for the purpose of decontamination and their field RGB sequences are well-overlapped.

Fig.9 shows the histogram of the number of MS stars per $arcmin^2$ at $r > 150''$ from the center of NGC 1978. The number of MS and He-Clump stars in this field have been subtracted from the NGC 1783 cluster stellar counts, after the normalization for the sampled area.

Hence, the total number of stars in each magnitude bin is given by:

$$N_{corr} = \frac{N_{obs}}{\phi} - N_{field}.$$

In order to compute the theoretical Φ_{norm} predicted by the PEL models, we have adopted the well-know technique of synthetic diagrams. By using the best-fit models described above, we randomly distributed the stars along the isochrone accordingly to a Salpeter initial mass function. An artificial dispersion has been added in order to simulate the photometric errors. For each model, 200 synthetic diagrams are computed by using Montecarlo simulations, and the corresponding Φ_{norm} are extracted and averaged together.

Fig. 10 (panel (a)) shows the observed LF (black points) compared with the theoretical expectations, computed by using the three different *overshooting* models. Clearly, the $\Lambda_{os}=0.0$ model predicts a Φ_{norm} value $\sim 10\text{-}15\%$ lower than the observed one; the $\Lambda_{os}=0.10$ and 0.25 models marginally ($<5\%$) underestimate the observed value of Φ_{norm} . This small offset can be easily accounted for by adding a binary population in the synthetic LF. To do this, we assumed that a given fraction f_b of the simulated stars be the primary star of a binary system. The mass of the primary is randomly extracted, while the mass of the secondary star is assigned by adopting the mass ratio q , between the secondary and primary star. The magnitude of the binary system is given by $M_{F555W}^{Binary} = -2.5 \cdot \log(10^{-2.5 \cdot (M_{F555W}^{prim} + M_{F555W}^{sec})})$, where M_{F555W}^{Binary} , M_{F555W}^{prim} , M_{F555W}^{sec} are the magnitudes of the binary, the primary and the secondary star, respectively. The latter has been obtained from the isochrone mass/luminosity relation. Panel (b) in Fig. 10 shows the comparison between the observed and theoretical Φ_{norm} with a binary population. The inclusion of $\approx 10\%$ binaries with a flat distribution of mass ratios ($q=0.80$) provide a good match between theoretical and observed Φ_{norm} for the models with overshooting. A residual discrepancy of $\approx 10\%$ is still present between the observed and the theoretical Φ_{norm} as predicted by the $\Lambda_{os}=0.00$ model. The adopted binary fraction is somewhat smaller than previous estimates ($\leq 30\%$) in other LMC and SMC clusters (Testa et al. 1995; Barmina, Girardi & Chiosi 2002; Chiosi & Vallenari 2007).

5. Discussion and Conclusions

The overall CMD characteristics of NGC 1783 are quite similar to those of NGC 1978 (Paper I), although there is evidence of an age difference. Indeed, we have shown that the best fit solutions to the observed CMD features are obtained by selecting $\Lambda_{OS}=0.1\text{-}0.25$ and $\tau=1.2\text{-}1.6$ Gyr for NGC 1783 (see Sect. 4) and $\Lambda_{OS}=0.1$ and $\tau=1.9$ Gyr for NGC 1978 (Paper I).

Further insight on the relative age of the two clusters can be obtained from the direct cluster-to-cluster comparison of the overall CMD properties. To this aim we can define the δV_{SGB}^{He-Cl} parameter as the magnitude difference between the luminosity distribution peak of the He-Clump and the flat region of the SGB. This *differential* parameter can provide an independent estimate of the age, and it is formally the analogous of the so-called *vertical method*, based on the magnitude difference between the TO and the Horizontal Branch magnitude level, and used to infer the age for the old globulars (see e.g. Buonanno, Corsi & Fusi Pecci 1989).

Fig. 11 shows the two observed CMDs with marked the δV_{SGB}^{He-Cl} parameter: we find $\delta V_{SGB}^{He-Cl} = 0.90$ and 1.56 for NGC1783 and NGC1978, respectively. This difference is an

independent, clearcut indication that NGC 1783 is younger than NGC 1978.

Fig. 12 shows the theoretical relations between the δV_{SGB}^{He-Cl} observable and the age, as derived from the PEL models with different amounts of *overshooting*. The grey area marked the region of the $(\tau, \delta V_{SGB}^{He-Cl})$ plane for a mild/strong overshooting efficiency appropriate for NGC 1783. Hence, by entering the measured δV_{SGB}^{He-Cl} in the above relations, an independent estimate of the age based on this differential parameter can be obtained.

By using the measured value of $\delta V_{SGB}^{He-Cl} = 0.90$, we find $\tau = 1.4 \pm 0.2 \pm 0.1$ Gyr for NGC 1783, where the first errorbar refers to the uncertainty in *overshooting* efficiency and the second to the uncertainties in the adopted reddening and distance modulus.

This age is still consistent with the one inferred by Geisler et al. (1997) ($\tau = 1.3$ Gyr), while it is significantly older than the age derived from the s-parameter ($\tau \sim 0.9$ Gyr) and by Mould et al. (1989) ($\tau = 0.7-1.1$ Gyr). Mucciarelli et al. (2006) note that the $N_{Bright-RGB}/N_{He-Cl}$ population ratio computed for NGC 1783 is too high for the clusters undergoing the RGB Phase-Transition, as suggested by the s-parameter age. Our new determination of an older age for NGC 1783, better reconcile the $N_{Bright-RGB}/N_{He-Cl}$ population ratio with the observed well-populated RGB.

Finally, we note that the structural parameters (r_c, r_t) and the age of the cluster inferred from this study, allow us to constrain the dynamical state of this cluster. The resulting core radius of $r_c = 24.5''$ (corresponding to ~ 5.9 pc adopting the distance modulus of $(m - M)_0 = 18.45$, obtained from the best-fit with the *overshooting* models (see Sect. 4)) is consistent with the age-core radius relationship discussed by Mackey & Gilmore (2003) and based on the surface brightness radial profiles of 53 LMC rich clusters. The youngest (ages $< \sim 200$ Myr) clusters of their sample exhibit core radii < 3 pc, while the older (both intermediate and old-age) stellar clusters show a more scattered distribution, with r_c between ~ 1 and ~ 8 pc, a major peak at $r_c \sim 2.5$ pc and the presence of several objects with $r_c > \sim 5$ pc. The inferred concentration parameter, $c = 1.16$, is consistent with a not core-collapse cluster (Meylan & Heggie 1997), as expected given the relatively young age of NGC 1783.

This research was supported by the Agenzia Spaziale Italiana (ASI) and the Ministero dell'Istruzione, dell'Università e della Ricerca.

REFERENCES

Alves, D. R., 2004, *New Astronomy Review*, 48, 659

- Barmina, R., Girardi, L., & Chiosi, C., 2002, *A&A*, 385, 847
- Becker, S., & Mathews, J., 1983, *AJ*, 270, 155
- Bedin, L. R., Cassisi, S., Castelli, F., Piotto, G., Anderson, J., Salaris, M., Momany, Y. & Pietrinferni, A., 2005, *MNRAS*, 357, 1048
- Bertelli, G., Nasi, E., Girardi, L., Chiosi, C., Zoccali, M., & Gllart, C., 2003, *AJ*, 125, 770
- Bessel, M. S., Castelli, F., & Plez, B., 1998, *A&A*, 333, 231
- Bohm-Vitense, E., 1958, *ZA*, 46, 108
- Brocato, E., Castellani, V., Ferraro, F. R., Piersimoni, A. M., & Testa, V., 1996, *MNRAS*, 282, 614
- Brocato, E., Di Carlo, E., & Menna, G., 2001, *A&A*, 374, 523
- Brocato, E., Castellani, V., Di Carlo, E., Raimondo, G., & Walker, A. R., 2003, *AJ*, 125, 3111
- Buonanno, R., Corsi, C. E., & Fusi Pecci, F. 1989, *A&A*, 216, 80
- Castellani, V., Degl’Innocenti, S., Marconi, M., Prada Moroni, P.G., Sestito, P., 2003, *A&A*, 404, 645
- Chiosi, E., & Vallenari, A., 2007, *A&A*, astro-ph/070228
- Elson, R. A., & Fall, S. M. 1985, *ApJ*, 299, 211
- Elson, R. A., 1992, *MNRAS*, 256, 515
- Ferraro, F.R., Fusi Pecci, F., Testa, V., Greggio, L., Corsi, C.E., Buonanno, R., Terndrup, D.M., & Zinnecker, H., 1995, *MNRAS*, 272, 391
- Ferraro, F. R., Origlia, L., Testa, V. & Maraston, C., 2004, *ApJ*, 608, 772
- Ferraro, F. R., Beccari, G., Rood, R. T., Bellazzini, M., Sills, A., & Sabbi, E., 2004, *ApJ*, 603, 127
- Ferraro, F. R., Mucciarelli, A., Carretta, E., & Origlia, L., 2006, *ApJ*, 645, L33
- Freytag, B., Ludwig, H.-G., & Steffen, M., 1996, *A&A*, 313, 497
- Fukunaga, K., 1972, "Introduction to statistical pattern recognition", Academic Press, New York

- Gallart, C., Zoccali, M., Bertelli, G., Chiosi, C., Demarque, P., Girardi, L., Nasi, E., Woo, J.-H., & Yi, S., 2003, *AJ*, 125, 742
- Geisler D., & Hodge, P., 1980, *ApJ*, 242, 73
- Geisler, D., Bica, E., Dottori, H., Claria, J. J., Piatti, A. E., & Santos, J. F. C. Jr., 1997, *AJ*, 114, 1920
- Girardi, L., Chiosi, C., Bertelli, G., & Bressan, A. 1995, *A&A*, 298, 87
- Iben, I., 1968, *Nature*, 220, 143
- Kerber, L., Santiago, B., & Brocato, E., 2007, *A&A*, 462, 139
- Mackey, A. D. & Gilmore, G. F., 2003, *MNRAS*, 338, 85
- Mackey, A. D. & Gilmore, G. F., 2004, *MNRAS*, 352, 153
- Mackey, A. D., Payne, M. J., & Gilmore, G. F., 2006, *MNRAS*, 369, 921
- Mackey, A. D., & Broby Nielsen, P., 2007, [astro-ph/0704336](https://arxiv.org/abs/astro-ph/0704336)
- Mateo, M., 1988, *ApJ*, 331, 261
- Meylan, G., & Heggie, D. C., 1997, *ARA&A*, 8, 1
- Montegriffo, P., Ferraro, F. R., Fusi Pecci, F., & Origlia, L., 1995, *MNRAS*, 276, 739
- Mould, J., & Aaronson, M., 1979, 1979, *BAAS*, 11, 719
- Mould, J., & Aaronson, M., 1982, *ApJ*, 263, 629
- Mould, J., Jerome, K., Nemec, J., Jensen, J., & Aaronson, M., 1989, *ApJ*, 339, 84
- Mucciarelli, A., Origlia, L., Ferraro, F. R., Maraston, C., & Testa, V., 2006, *ApJ*, 646, 939
- Mucciarelli, A., Ferraro, F. R., Origlia, L., & Fusi Pecci, F., 2007, *AJ*, 133, 2053
- Olsen, K. A. G., Hodge, P. W., Mateo, M., Olszewski, E. W., Schommer, R. A., Suntzeff, N. B., & Walker, A. R., 1998, *MNRAS*, 300, 665
- Origlia, L., & Leitherer, C., 2000, *AJ*, 119, 2018
- Persson, S. E., Aaronson, M., Cohen, J. G., Frogel, J. A., & Matthews, K., 1983, *ApJ*, 266, 105

- Salaris, M., Chieffi, A., & Straniero, O., 1993, *ApJ*, 414, 580
- Searle, L., Wilkinson, A., & Bagnuolo, W. G. 1980, *ApJ*, 239, 803
- Sigurdsson, S., & Phinney, E. S., 1995, *ApJS*, 99, 609
- Stetson, P. B., 1987, *PASP*, 99, 191
- Testa, V., Ferraro, F. R., Brocato, V., & Castellani, V., 1995, *MNRAS*, 275, 454.
- Testa, V., Ferraro, F. R., Chieffi, A., Straniero, O., Limongi, M., & Fusi Pecci, F., 1999, *AJ*, 118, 2839
- Vallenari, A., Aparicio, A., Fagotto, F., & Chiosi, C., 1994, *AJ*, 284, 424
- van den Bergh, S., 1981, *A&AS*, 46, 79

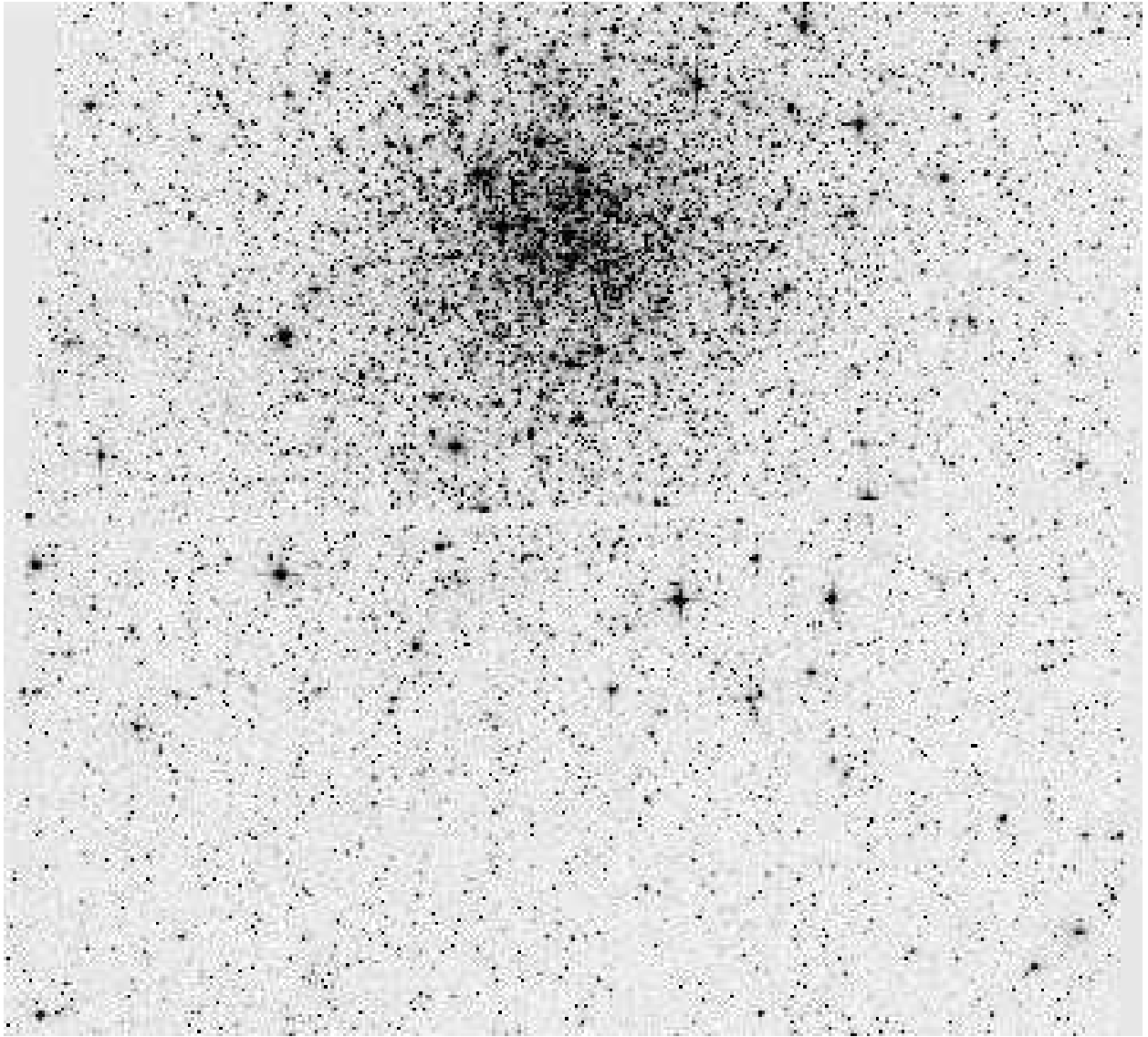


Fig. 1.— ACS/WFC F814W image of the LMC cluster NGC 1783, both two chips.

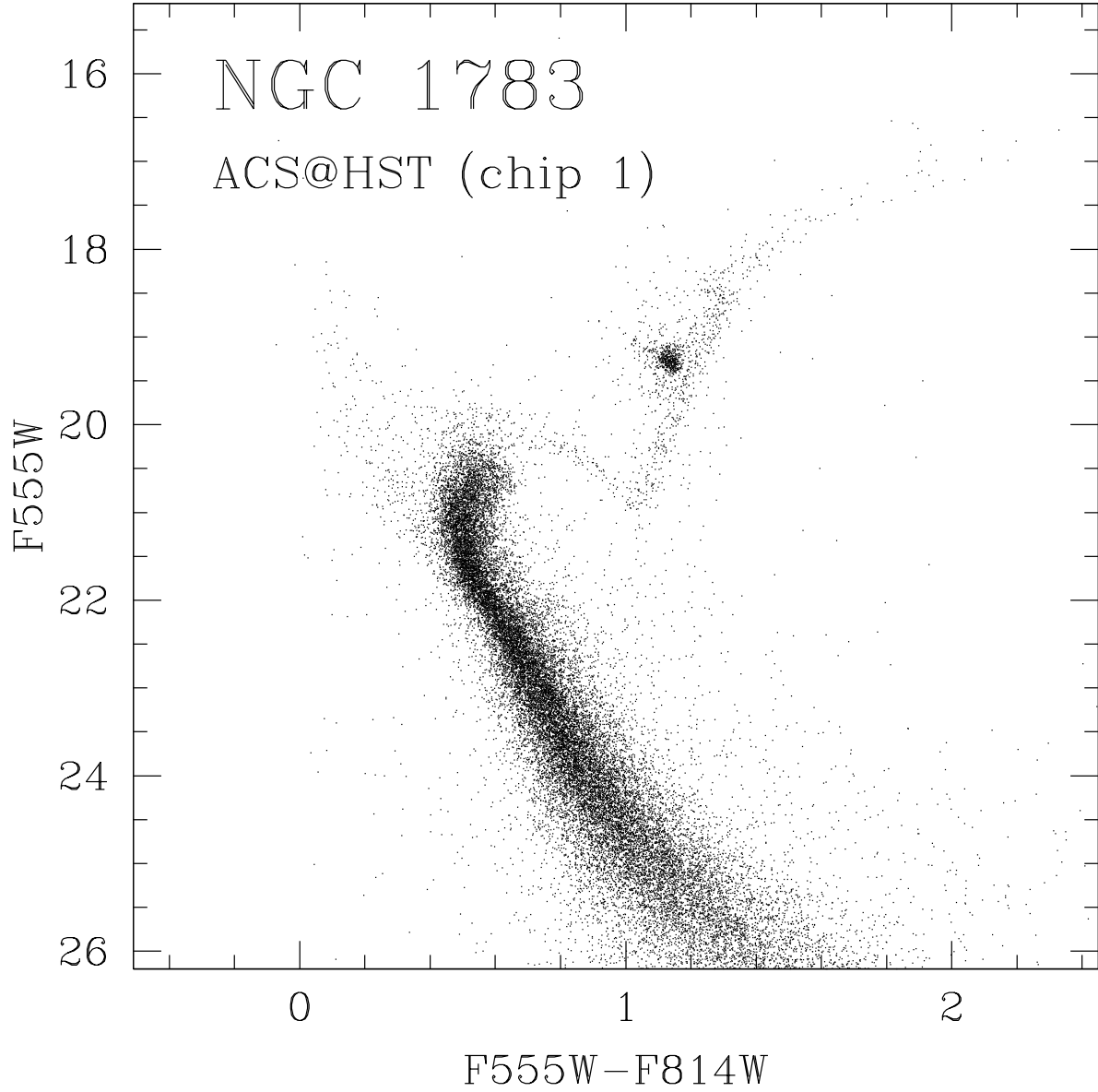


Fig. 2.— (F555W, F555W-F814W) CMD of the LMC cluster NGC 1783, obtained with ACS@HST (only stars lying into the chip containing the cluster core have been plotted).

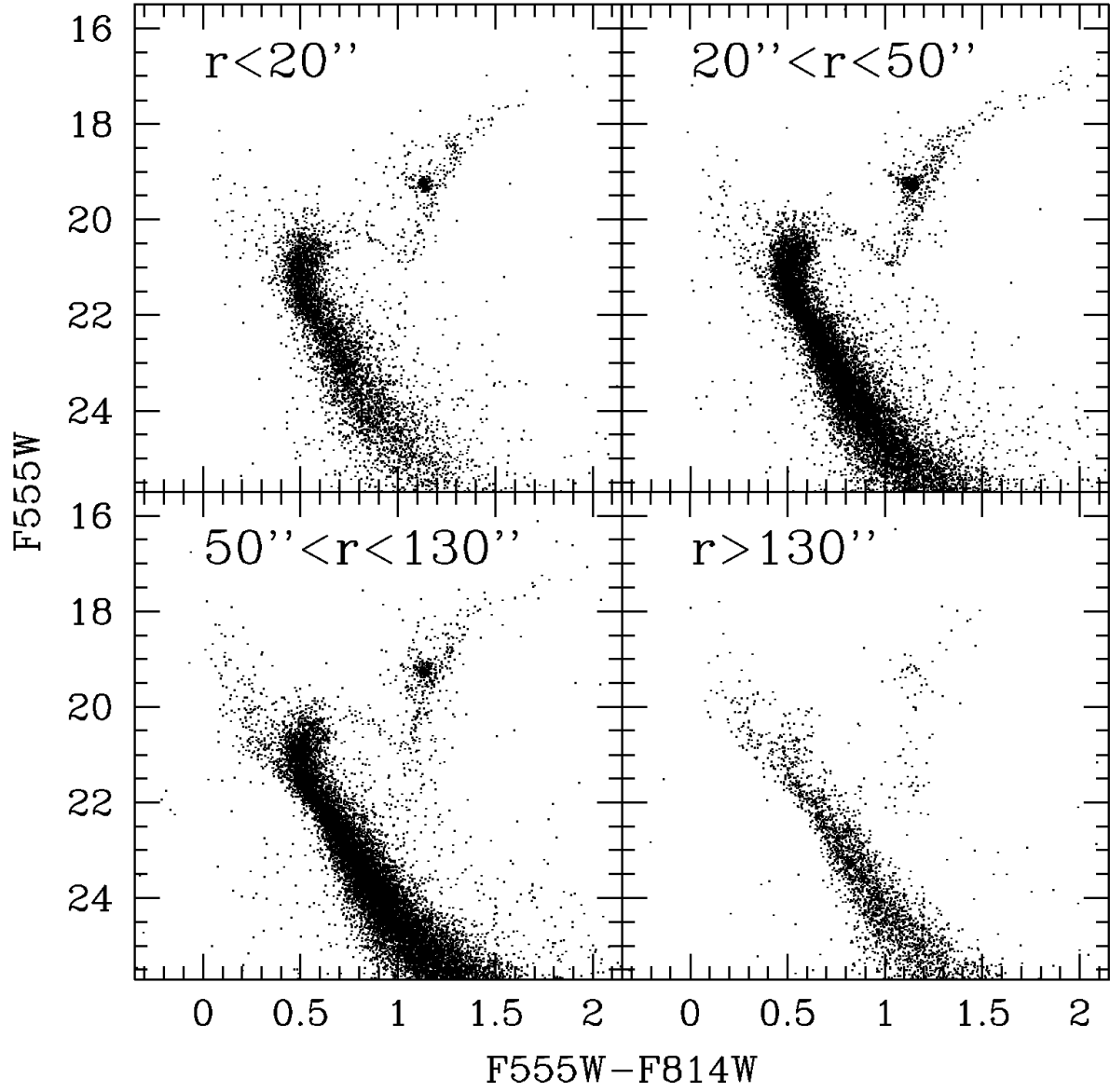


Fig. 3.— Radial (F555W ,F555W-F814W) CMD of NGC 1783 at increasing distances from the cluster center.

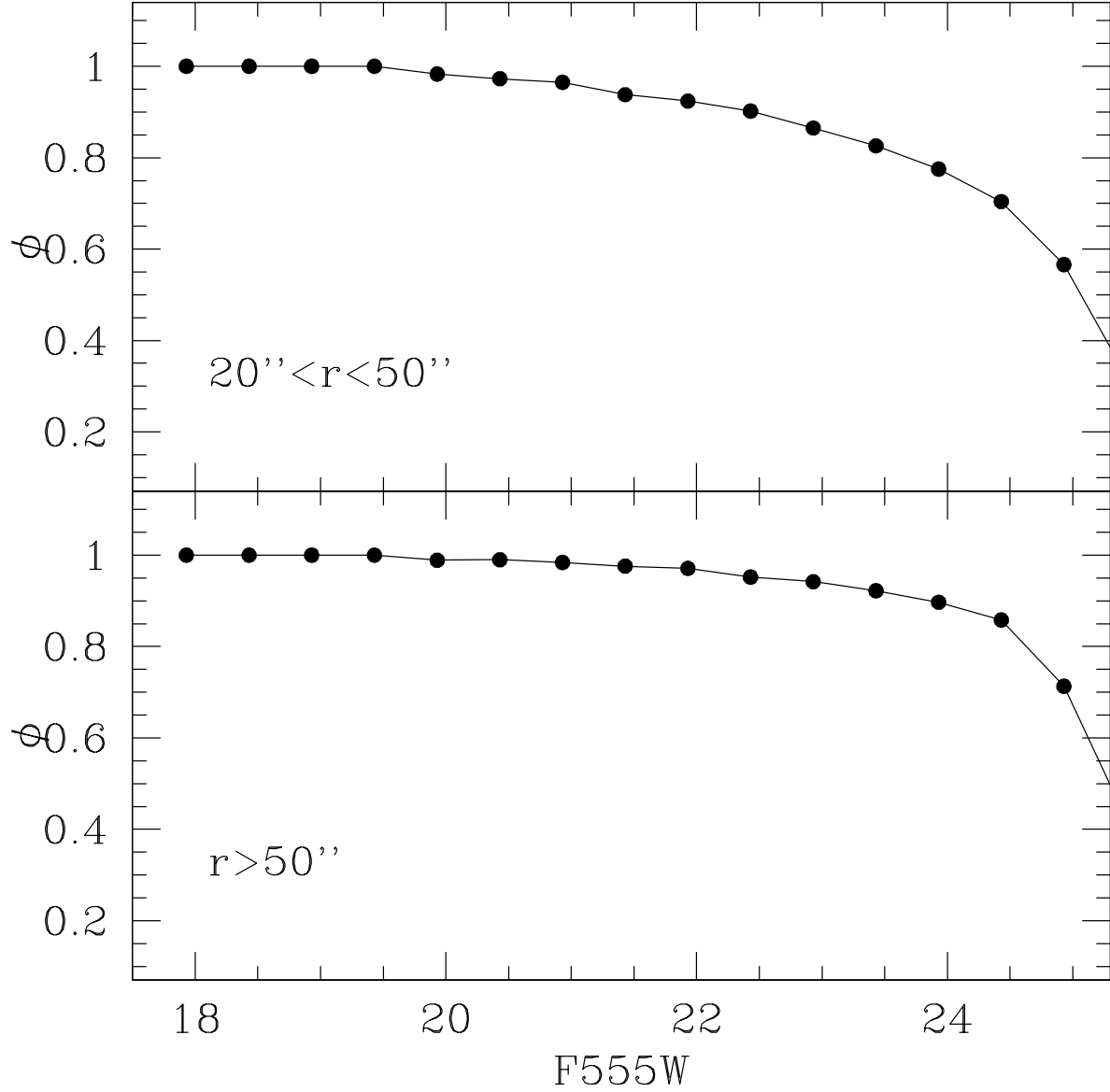


Fig. 4.— Completeness curves computed in two radial sub-regions of NGC 1783. The black points indicate the value of the $\phi = \frac{N_{rec}}{N_{sim}}$ parameter calculated for each 0.5 magnitude bin.

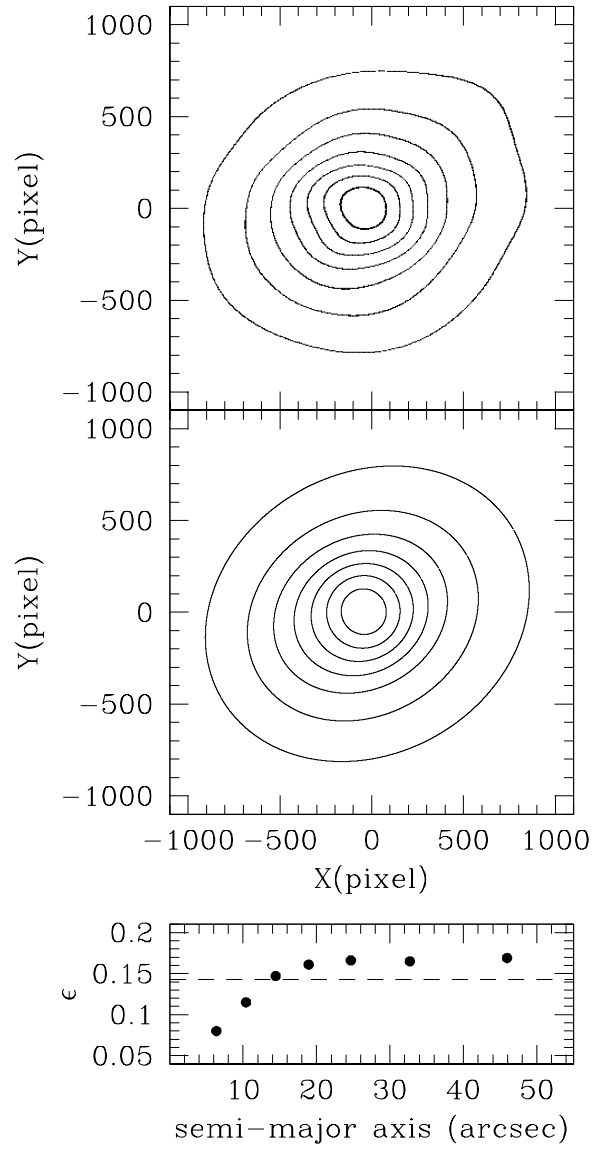


Fig. 5. *Upper panel:* the map of NCC 1782 with the isodensity contours; *central panel:*

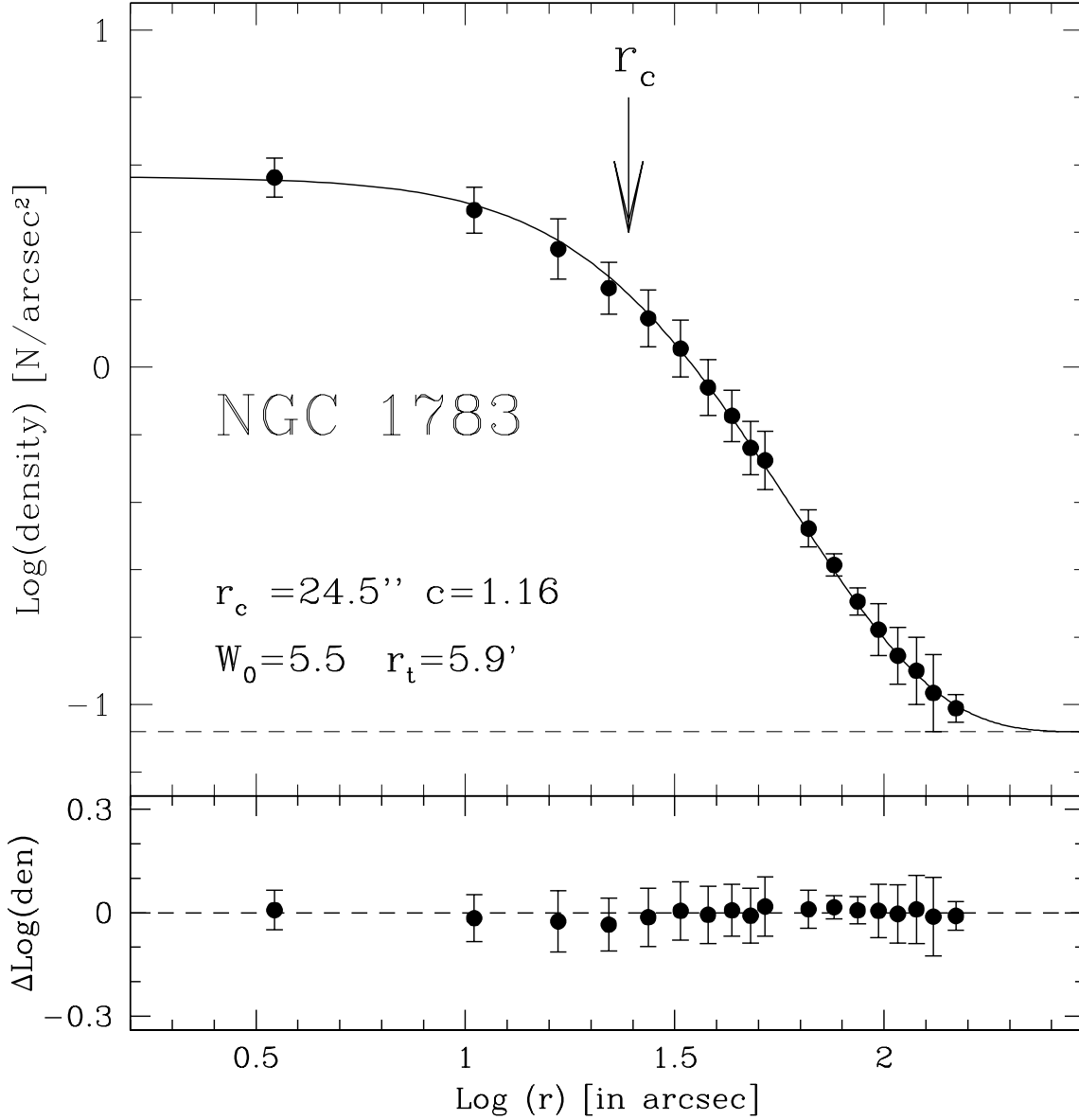


Fig. 6.— *Upper panel*: observed radial density profile for the cluster NGC 1783. The solid line is the best fit King model, with $r_c=24.5''$ and $c=1.16$. The *horizontal dashed line* indicate the background level. *Lower panel*: the χ^2 test for the observed radial density profile and best-fit King model (solid line).

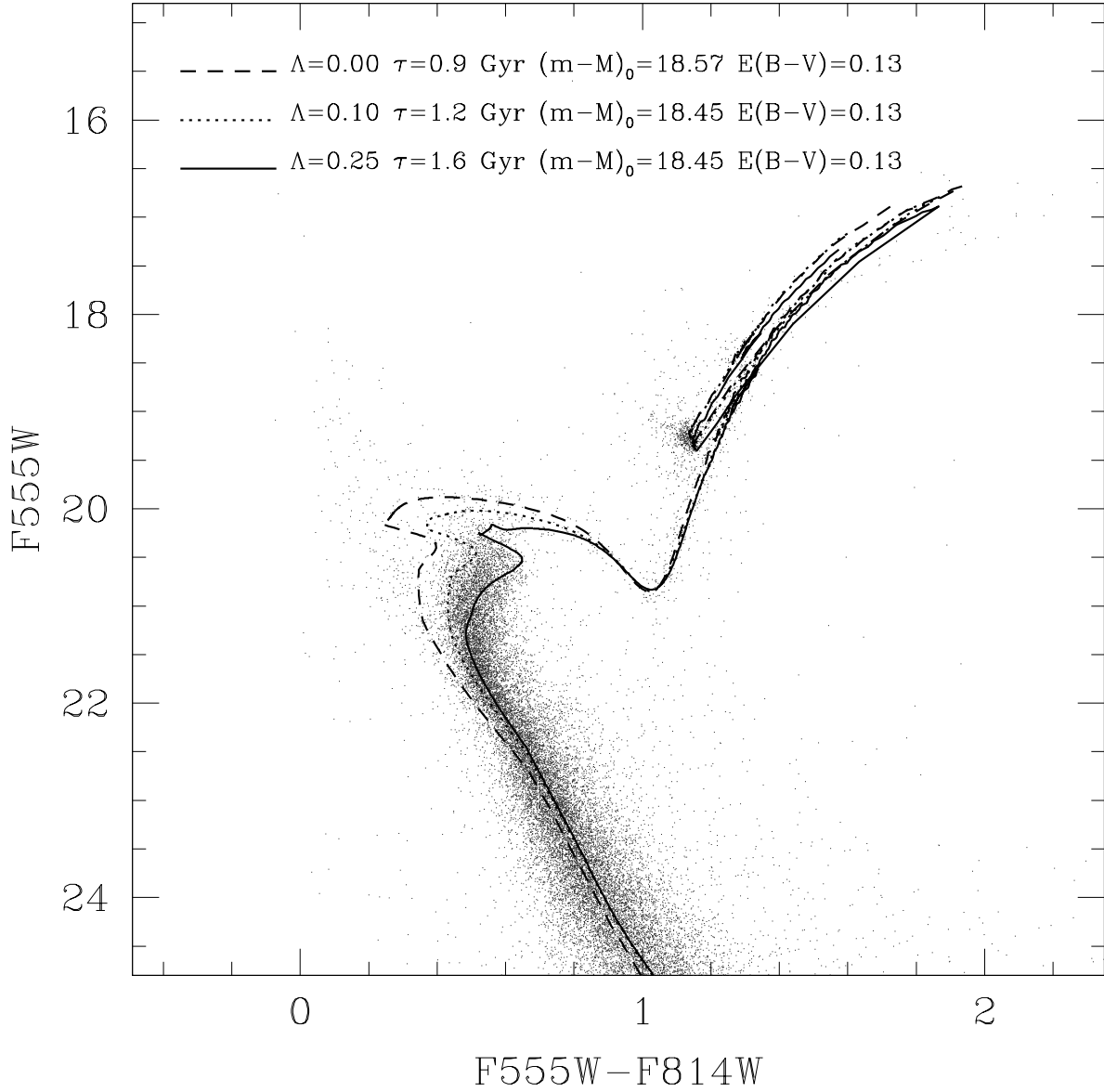


Fig. 7.— Best-fit theoretical PEL isochrones overplotted on the observed CMD of NGC 1783. Models with different assumptions of the overshooting efficiency (Λ_{os}) are used: the best fit age, distance modulus and reddening (see text) for each choice of Λ_{os} are also marked.

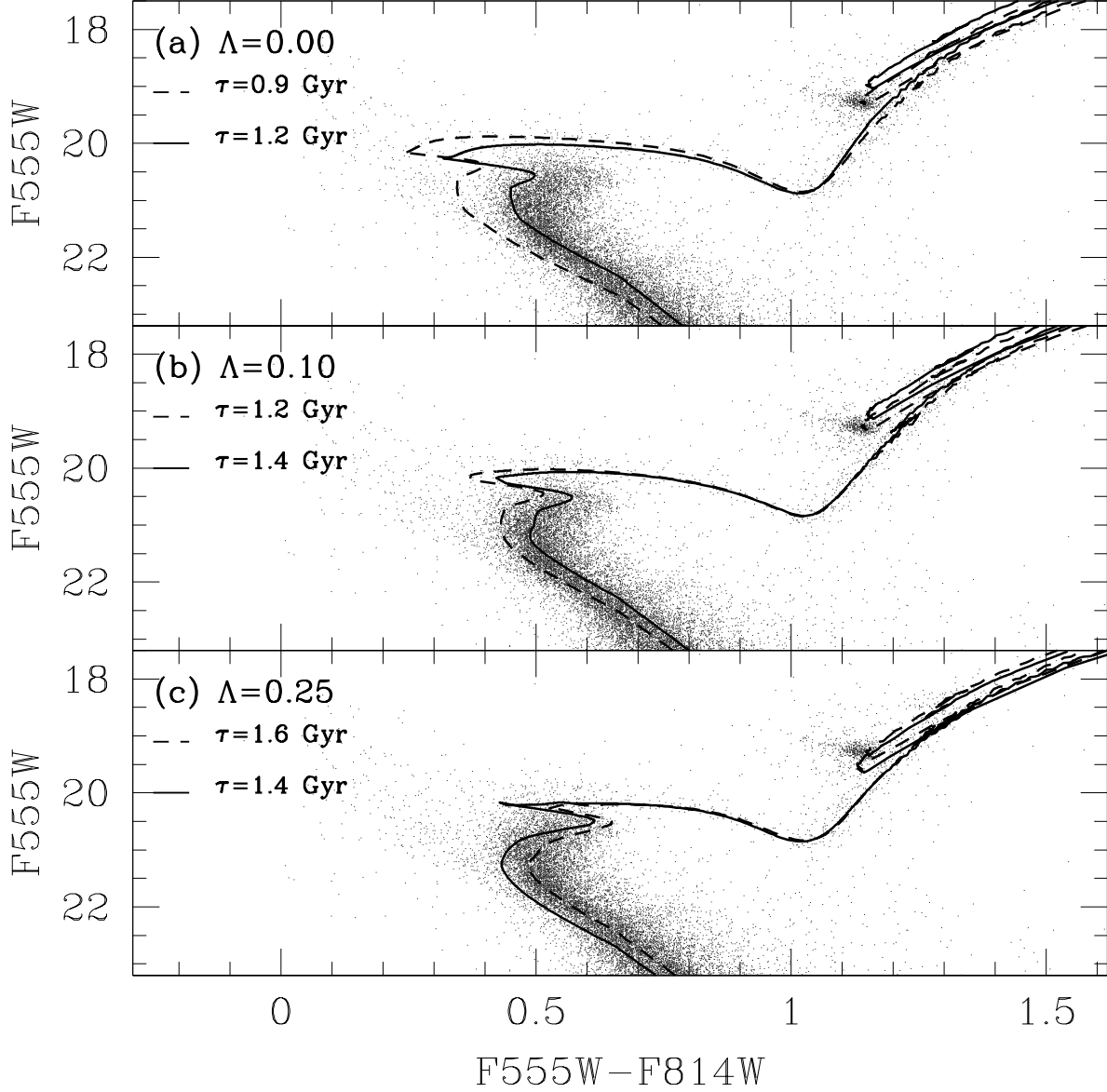


Fig. 8.— Portion of the CMD, as zoomed onto the TO region, with different models overplotted. Panel (a): best-fit (dashed line, $\tau=0.9$ Gyr, $(m - M)_0=18.45$) and older (solid line, $\tau=1.2$ Gyr, $(m - M)_0=18.16$) isochrones for $\Lambda_{os}=0.00$. Panel (b): best-fit (dashed line, $\tau=1.2$ Gyr, $(m - M)_0=18.45$) and older (solid line, $\tau=1.4$ Gyr, $(m - M)_0=18.25$) isochrones for $\Lambda_{os}=0.10$. Panel (c): best-fit (dashed line, $\tau=1.6$ Gyr, $(m - M)_0=18.45$) and younger (solid line, $\tau=1.4$ Gyr, $(m - M)_0=18.66$) isochrones for $\Lambda_{os}=0.25$.

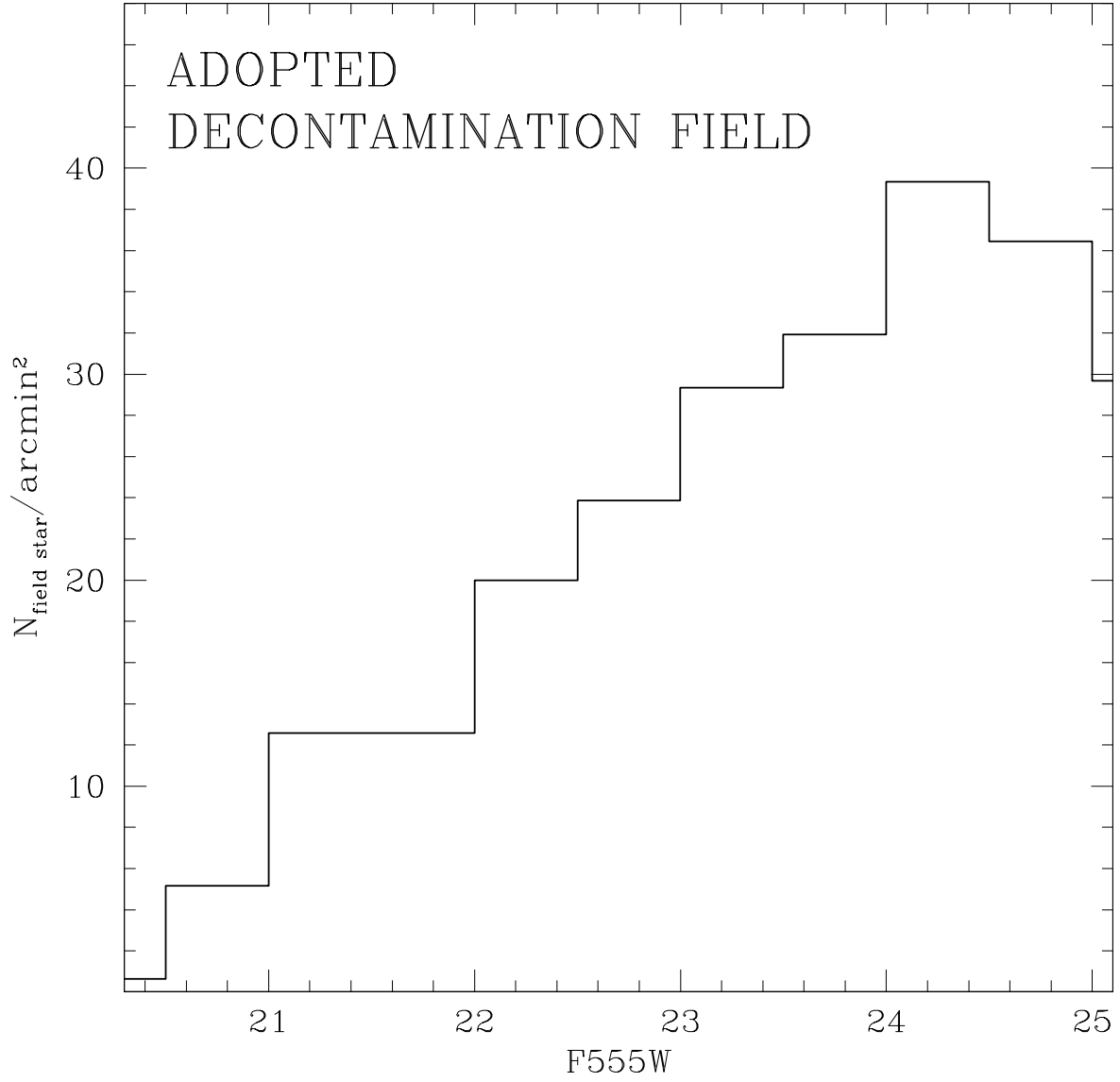


Fig. 9.— Histogram of the number of MS stars per arcmin^2 at $r > 150''$ from the center of NGC 1978.

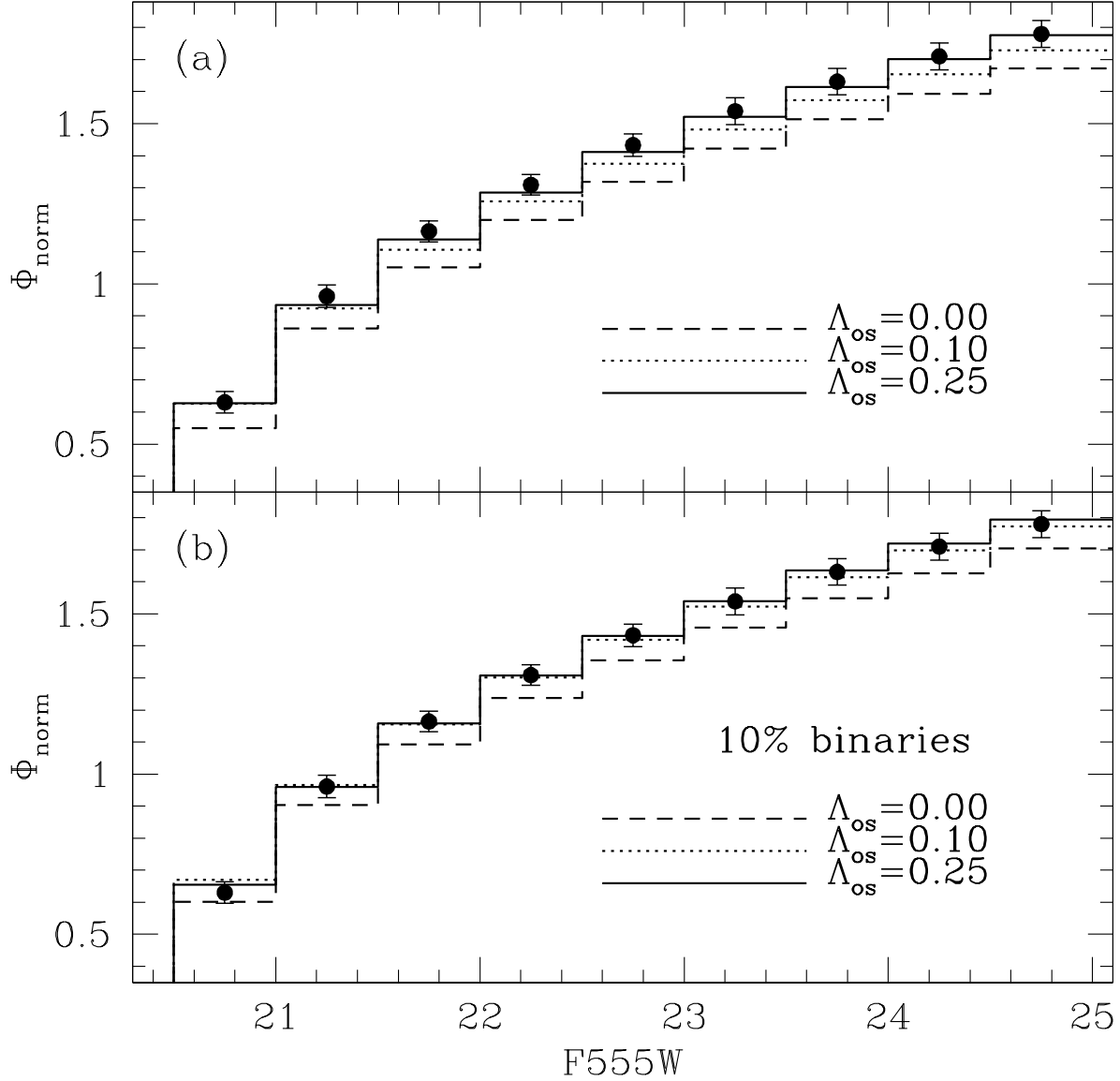


Fig. 10.— Panel (a): integrated LF of the MS stars normalized to the number of He-Clump stars: *black points* indicate the observed LF and their size correspond to their typical uncertainty. The three line are the theoretical LFs computed by adopting $\Lambda_{\text{os}}=0.0$ (dashed), 0.10 (dotted) and 0.25 (continuous). Panel (b): same as panel (a), but adding a 10% binary fraction in the computation of the theoretical LFs.

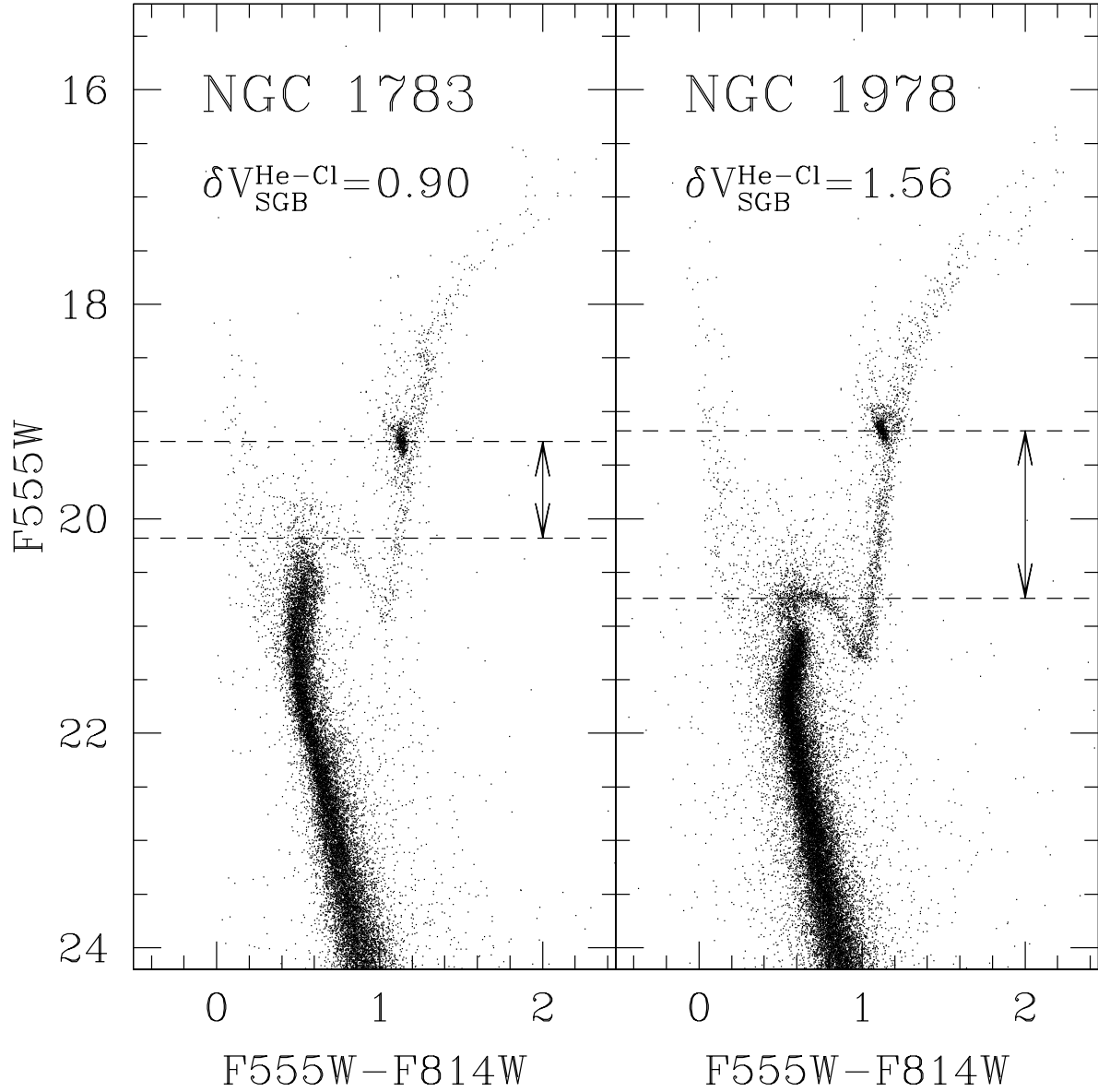


Fig. 11.— ACS@HST (F555W, F555W-F814W) CMDs for the LMC cluster NGC 1783 (left panel) and NGC 1978 (right panel). The arrows indicate the magnitude difference $\delta V_{\text{SGB}}^{\text{He-Cl}}$ between the He-Clump and the flat portion of the SGB.

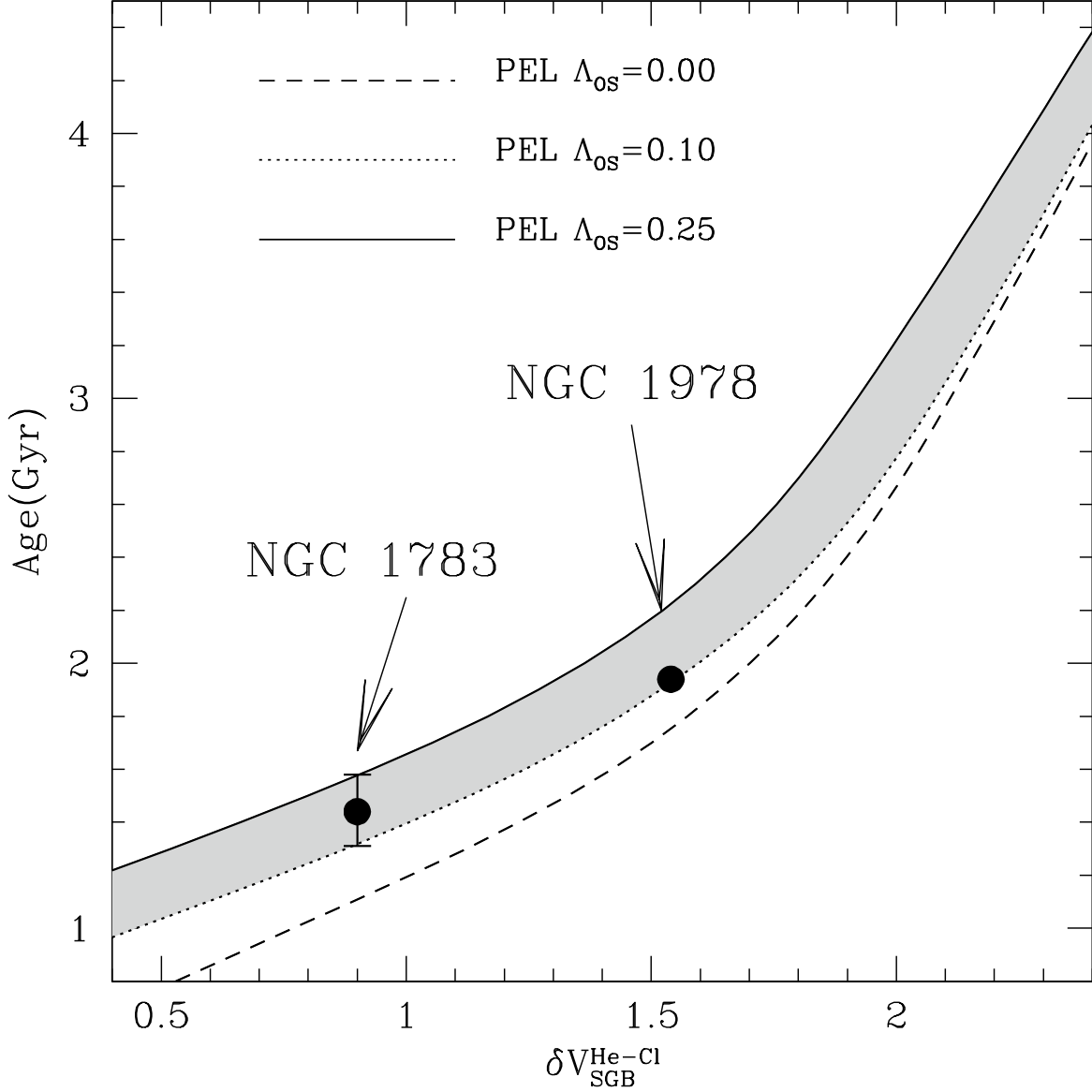


Fig. 12.— Theoretical predictions for the magnitude difference between the He-Clump and the flat portion of the SGB as a function of the age for three different *overshooting* assumptions: $\Lambda_{OS}=0.0$ (dashed line), $\Lambda_{OS}=0.10$ (dotted line) and $\Lambda_{OS}=0.25$ (solid line). The observed values for δV_{SGB}^{He-Cl} and the inferred ages for NGC 1783 (this paper) and NGC 1978 (Paper I) are plotted as black points.